Waterborne electrospinning of poly(*N*-isopropyl acrylamide) by control of environmental parameters

Ella Schoolaert[a], Paulien Ryckx[b], Jozefien Geltmeyer[a], Samarendra Maji[c], Paul H.M. Van Steenberge[b], Dagmar R. D'hooge[a;b], Richard Hoogenboom[c] and Karen De Clerck*[a]*

[a] Centre for Textile Science and Engineering (CSTE), Department of Materials, Textiles and Chemical Engineering, Faculty of Engineering and Architecture, Ghent University (UGent), Technologiepark 907, 9052 Ghent, Belgium – +32 (0)9 264 57 40 – karen.declerck@ugent.be

[b] Laboratory for Chemical Technology (LCT), Department of Materials, Textiles and Chemical Engineering, Faculty of Engineering and Architecture, Ghent University (UGent), Technologiepark 914, 9052 Ghent, Belgium

[c] Supramolecular Chemistry Group, Department of Organic and Macromolecular Chemistry, Faculty of Sciences, Ghent University (UGent), Krijgslaan 281 S4, 9000 Ghent, Belgium – +32 (0)9 264 44 82 – richard.hoogenboom@ugent.be

*Corresponding authors: Karen.DeClerck@ugent.be; Richard.Hoogenboom@ugent.be

Keywords

Poly(N-isopropyl acrylamide), aqueous media, electrospinning, nanofibers, Lower Critical Solution Temperature, rheology

Abstract

With increasing toxicity and environmental concerns, electrospinning from water, *i.e.* waterborne electrospinning, is crucial to further exploit the resulting nanofiber potential. Most water-soluble polymers have the inherent limitation of resulting in water-soluble nanofibers and a tedious chemical cross-linking step is required to reach stable nanofibers. An interesting alternative route is the use of thermoresponsive polymers, such as poly(N-isopropyl acrylamide) (PNIPAM), as they are water-soluble beneath their lower critical solution temperature (LCST) allowing low temperature electrospinning while the obtained nanofibers are water-stable above the LCST. Moreover, PNIPAM nanofibers show major potential to many application fields, including biomedicine, as they combine the well-known on-off switching behavior of PNIPAM, thanks to its LCST, with the unique properties of nanofibers. In the present work, based on dedicated turbidity and rheological measurements, optimal combinations of polymer concentration, environmental temperature and relative humidity are identified allowing, for the first time, the production of continuous, bead-free PNIPAM nanofibers electrospun from water. More specifically, PNIPAM gelation was found to occur well below its LCST at higher polymer concentrations leading to a temperature regime where the viscosity significantly increases without compromising the polymer solubility. This opens up the ecological, water-based production of uniform PNIPAM nanofibers that are stable in water at temperatures above PNIPAM's LCST, making them suitable for various applications, including drug delivery and switchable cell culture substrates.

1 Introduction

Poly(N-isopropyl acrylamide) or PNIPAM is a well-known and commonly applied polymer in biomedical applications as its Lower Critical Solution Temperature (LCST) of *ca.* 30-35 °C in water is beneficial for use in drug delivery and cell culture.[1–11] As this thermoresponsivity can be interpreted as a 'smart' behavior, PNIPAM has also been used for the development of novel coatings and sensor materials.[1,3,6,7,12–17] Below the LCST, hydrogen bonds are present between water molecules and the hydrophilic regions of the polymer chains, resulting in excellent water-solubility of PNIPAM. Yet, if the temperature is raised above the LCST, it becomes thermodynamically more favorable for the hydrating water molecules to go back to the bulk water, which is an entropic effect. As a result, the partially dehydrated PNIPAM chains become water insoluble and agglomerate.[7,18–23]

For several applications, including drug delivery, PNIPAM has mainly been applied as a gel or as part of a micellar structures, where a (medical) substance can be captured inside.[3,4,7,11] When an external stimulus causes the temperature to cross the LCST, the gel or micelle structure changes its physical structure, which releases the substance. This on-off switching behavior is also being used for cell culture.[2,3,24–26] Many literature studies report the successful attachment and proliferation of cells onto PNIPAM scaffolds after which the produced cell sheet is easily removed by simply cooling the PNIPAM support below its LCST.[2,3,24–26] Although this concept has shown major potential already, there is still need for improvement.[27,28]

For many applications a highly porous, open and flexible structure with a large specific surface area is also desired.[27–33] Nanofibrous membranes have already proven their potential for numerous applications requiring a high sensitivity, porosity, and specific surface area as well as versatility and easy functionalization.[28,31,34–39] Their resemblance to the extracellular matrix makes nanofibers

also ideally suited for biomedical applications, *e.g.* tissue engineering and drug delivery.[27,28,31–33,40,41]

These nanofibrous membranes are ideally fabricated by solvent-electrospinning in which nanofibers are drawn from a viscous polymer solution toward a collector plate, due to the application of an electrical field.[42,43] Since current solvent-electrospinning is mainly based on the use of strong acids and/or toxic solvent systems, increasing environmental concerns demand a switch to waterborne electrospinning, *i.e.* electrospinning from water, to provoke industrial growth.[44–47] Clearly, waterborne electrospinning is a major advantage for biomedical applications, as harmful or toxic solvent traces are prevented.

Thermoresponsive polymers, such as PNIPAM, are appealing materials for waterborne electrospinning as their LCST-behavior enables nanofiber production from water below the LCST transition, yet provides water stability during application above the LCST transition. However, this option has barely been investigated and if considered only with limited success. Previous studies report very poor PNIPAM electrospinnability from water and required a combined, harsher solvent system, *e.g.* acetone or toxic solvents such as DMF and THF[45,48–52], or the use of copolymers where another polymer is introduced in order to facilitate the electrospinning process.[53–58] It should, however, be highlighted that – to the best of our knowledge – none of these studies have fully exploited the LCST behavior to enhance the electrospinnability of PNIPAM. In general, ambient parameters such as the environmental temperature and relative humidity have not been considered. Yet, it can be expected that tuning of these parameters will be crucial for the processability of a thermoresponsive polymer such as PNIPAM.

Therefore, in the present work, the influence of both the environmental temperature and relative humidity is studied thoroughly, hereby fully exploiting the thermoresponsive behavior of PNIPAM

to enhance electrospinnability from water. Based on the common insight that a certain viscosity and good solubility are required for a stable electrospinning process, systematic rheological analysis and turbidimetry measurements are employed to study the effect of temperature control. Additionally, the identification of the optimal relative humidity is facilitated and supported by detailed Dynamic Vapor Sorption (DVS) analysis.

It is, thus, aimed to process PNIPAM into continuous, uniform, bead-free nanofibrous mats using only water as the solvent. This will provide the first clean and environmental-friendly, fully water-based fabrication method for PNIPAM nanofibers with water-stability at the temperature of the human body, which makes them appealing for many fields including biomedicine.

2 Experimental Section

2.1 Materials

PNIPAM with a viscosity average molar mass of *ca.* $3 \cdot 10^5$ g·mol^{-1} was purchased from Scientific Polymer Products, Inc. (Ontario, NY) and used as received. The dispersity of the commercial PNIPAM was determined as 4.2 with size exclusion chromatography (SEC). SEC was performed on an Agilent 1260-series HPLC system equipped with a 1260 online degasser, a 1260 ISO-Pump, a 1260 automatic liquid sampler, a thermostatted column compartment, a 1260 diode array detector (DAD) and a 1260 refractive index detector (RID). Analyses were performed on a PPS Gram30 column in series with a PPS Gram 1000 column at 50 C. DMA containing 50 mM of LiCl was used as an eluent at a flow rate of 0.6 mL/min. The SEC traces were analyzed using the Agilent Chemstation software with the GPC add on. Molar mass and PDI values were calculated against polymethylmethacrylate standards. The distilled water used in this work was of type III as considered in ISO 3696, having a conductivity below 0.5 μS cm^{-1}. Fluorescein was obtained from Sigma Aldrich and used as received.

2.2 Electrospinning

Electrospinning solutions were prepared under acclimatized conditions in a Weiss WK-340/40 climate chamber at 15 °C, unless stated otherwise, by dissolving a specific amount of PNIPAM in water. For the preparation of the fluorescein-doped nanofibers, fluorescein was first dissolved in acetone (8.5 mg/ml) and subsequently added to a 10 wt% aqueous PNIPAM solution to achieve a concentration of 0.5 wt% fluorescein on polymer mass. Mass concentrations are expressed by weight percentages (wt%) defined by the ratio of the polymer mass and the sum of the polymer and solvent mass. The (dynamic) viscosity of the solutions was determined using a Brookfield viscometer LVDV-II (spindle S18, viscosity range of 1.5 - 3.0 10^5 mPa·s, average error of 8%).

All electrospinning experiments were carried out on a mononozzle setup using the solvent electrospinning technique with an 18 gauge Terumo mixing needle without bevel. A stable Taylor cone was achieved at a flow rate of 0.5 $ml \cdot h^{-1}$, selecting a tip-to-collector distance of 25 cm, and applying a voltage between 15-20 kV. Electrospinning was always performed in the climate chamber, as to properly adjust the environmental temperature and relative humidity. It should be noted that, at a relative humidity of 25 ± 5 %RH, the temperature could not be set below 17 °C, which is therefore a limiting temperature. After electrospinning, the produced nanofibrous samples were dried in an oven below the onset of the Tg of PNIPAM, *i.e.* 130 °C (ESI Figure S1), as to remove all remaining water. This drying procedure did not alter the nanofiber morphology compared to samples that were dried at lower temperatures, *e.g.* 80 °C, or compared to samples that were not dried (ESI Figure S2). The nanofibrous membranes were stored in a desiccator.

2.3 Characterization

All nanofibrous samples were analyzed by an FEI Quanta 200 FFE-SEM at an accelerating voltage of 20 kV. Samples were prepared prior to analysis by applying a gold coating using a

sputter coater (Balzers Union SKD 030). The nanofiber diameters were measured using ImageJ. The average diameters and their standard deviations were based on 50 measurements per sample.

Water stability of the produced nanofibers was tested by immersion of the samples in water on a heating plate as to keep the temperature of the water constant at 37 °C or 50 °C, being above the LCST of PNIPAM. Below these temperatures, the nanofibers are always completely dissolved, as expected. After immersion of either 30 seconds or 5 minutes, the water was removed from the samples by a syringe while the samples were kept on the heating plate as long as there was still water present in order to avoid the remaining water to cool down below the LCST of PNIPAM. The samples were subsequently dried by four different drying procedures, *i.e.* drying in a vacuum oven at 50 °C, drying in a climate chamber at 50 °C and 15 %RH, drying in a desiccator and drying on a well-controlled heating plate at 50 °C or 90 °C. The SEM images given in this paper result from the latter drying process since all drying procedures led to the same nanofiber morphology (ESI Figure S3).

Vapor desorption measurements were carried out with a Q5000SA Dynamic Vapor Sorption (DVS) apparatus from TA Instruments. Samples of 9.00 ± 0.50 mg were characterized by using metalized quartz sample pans. The experiments always started after a 5 minutes stabilization step at 20 °C and 98 %RH, after which the temperature and/or relative humidity was equilibrated to the actual set point. All mass changes were allowed to reach equilibrium (mass change < 0.05 % during 60 minutes).

Rheological measurements to grasp the relevance of physical crosslinking and gel formation were performed on an MCR 302 Anton Paar rheometer with a Peltier CTD 180 heating equipment. 2 ml of each solution was pressed between a profiled, lower measuring plate and a parallel rotating measuring plate with a diameter of 50 mm. Prior to recording the actual data, frequency and

amplitude sweeps were carried out as to select a suitable working frequency and amplitude allowing a sufficient differentiation of the elastic and viscous part over a broad temperature window; values of 0.5 Hz and 0.2 %, respectively, resulted. For each experiment, a linear temperature ramp from 10 °C to 40 °C at 1° per min was established. Each 30 seconds, a data point was taken, allowing a measurement of the loss modulus, storage modulus and complex viscosity as a function of temperature. In agreement with literature data, this allows to determine the gel point in two consisting manners, *i.e.* the identification of the largest change in the complex viscosity and the crossover of the loss and storage modulus.[59–61]

Cloud point determination was carried out by turbidimetry on an Avantium Crystal 16 turbidimeter. 1 ml of each solution was examined according to cycling the temperature in between 10 °C and 40 °C and the cloud point temperatures (T_{CP}'s) were determined as the temperature at which the transmission had lowered to 50% during heating. As to account for the heating rate effect[23], different heating rates (0.2 K/min, 0.5 K/min, 1 K/min and 2 K/min) were applied. Similar results were obtained for the different heating rates, however, only the results corresponding to 0.5 K/min are presented in this article as recently recommended.[62]

Modulated temperature DSC traces were analyzed with a TA Instruments Q2000, equipped with a refrigerated cooling system (RCS90) and using nitrogen as purge gas (50 $ml \cdot min^{-1}$). The instrument was calibrated using Tzero™ technology for standard Tzero aluminum pans using indium at the heating rate used during the measurement. The heating rate was set at 2 °/min and samples of 2.5 ± 0.5 mg were used. The selected temperature modulation was ± 0.5 °C every 40 seconds. The samples were analyzed *via* two heating cycles in which they were heated from 0 °C to 250 °C.

The fluorescence of the fluorescein-doped nanofibers was analyzed with a Cary Eclipse fluorescence spectrophotometer. The emission spectra result from excitation at 450 nm with a photomultiplier tube voltage of 470 V and a slit width of 10 nm for both excitation and emission.

3 Results and discussion

In this section, it is first illustrated that a waterborne electrospinning of PNIPAM requires control of the solution temperature and relative humidity, considering turbidity, rheological and DVS data. Based on the obtained insights, the optimal processing window is subsequently identified for the production of stable PNIPAM nanofibers. By performing water stability tests the latter is further confirmed.

3.1 Relevance of temperature control

In general, the polymer solubility is one of the main requirements for stable solvent electrospinning.[34,42,43] In the case of waterborne electrospinning of PNIPAM, this means that the initial processing or solution temperature needs specific attention as PNIPAM is only water soluble beneath its LCST. Many literature studies have investigated the LCST behavior of PNIPAM and the phase diagrams as measured by turbidimetry in this work, are in agreement with previous studies.[60,63–67] The temperature of demixing or the T_{CP} is often taken as an indicative for the LCST transition. From Figure 1, it can be concluded that the initial processing temperature of PNIPAM in water should be kept well below 30°C in order to have clear solutions, allowing to create uniform, bead-less nanofibers.

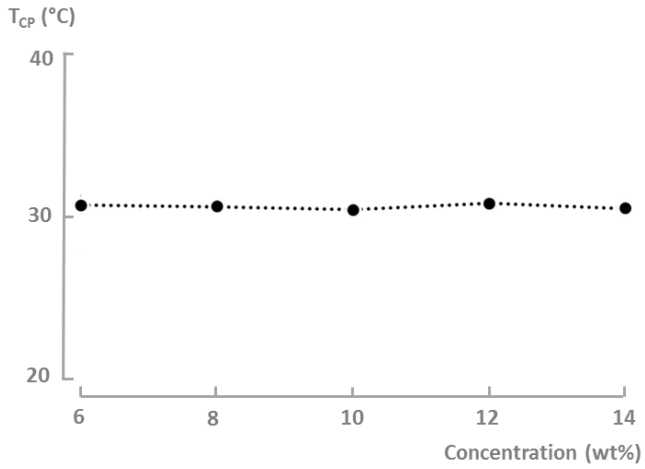

Figure 1. Cloud point temperature (T_{CP}) of PNIPAM in water as function of concentration determined by turbidimetry confirms the LCST of PNIPAM of *ca*. 31 °C.

Another key parameter for solvent electrospinning is the (dynamic) viscosity of the polymer solution as this is an indicative for the amount of chain entanglements, which are needed for the formation of nanofibers upon processing. As PNIPAM undergoes partial dehydration leading to agglomeration and physical crosslinking during the LCST transition, the viscosity is expected to increase drastically around this temperature. Table 1, indeed, illustrates an increased solution viscosity with increasing temperature at various electrospinning mass concentrations.

Table 1. List of the electrospinning mass concentrations with viscosity clearly depending on the solution temperature.

Concen-tration	Dissolved at 15 °C Viscosity (mPa.s)	Dissolved at 25 °C Viscosity (mPa.s)	Relative values**
6 wt%	$1.0 \cdot 10^2$	$1.4 \cdot 10^2$	1.4
8 wt%	$2.9 \cdot 10^2$	$8.0 \cdot 10^2$	2.8
10 wt%	$9.2 \cdot 10^2$	$6.0 \cdot 10^3$	6.5
12 wt%	$2.0 \cdot 10^3$	$> 3.0 \cdot 10^{5*}$	> 150
14 wt%	$7.1 \cdot 10^3$	$>> 3.0 \cdot 10^{5*}$	>> 150

*Viscosity values were higher than the apparatus' limit, being $3.0 \cdot 10^5$ mPa·s
**Relative values are calculated as the ratio of the viscosities of the polymer solutions dissolved at 25 °C and dissolved at 15 °C as to illustrate the increase in viscosity upon increasing temperature

Of course, at a given temperature the viscosity also increases with increasing polymer concentration, yet, at higher polymer concentrations, the temperature effect is more pronounced (see last column; ratio of the viscosity values). Strikingly, while the T_{CP} of PNIPAM is hardly affected by the polymer concentration (Figure 1), the viscosity at 25 °C and the ratio of the viscosity at 25 °C and 15 °C increases tremendously.

A more thorough analysis of the effect of temperature on the solution viscosity is further performed by rheological measurements in which the temperature is gradually increased and the viscoelastic change is recorded by measuring the loss and storage modulus and the related complex viscosity.

The complex viscosity was used to analyze the physical crosslinking profile as it directly takes into account both the variation of the storage modulus and loss modulus (Figure 2).[59–61]

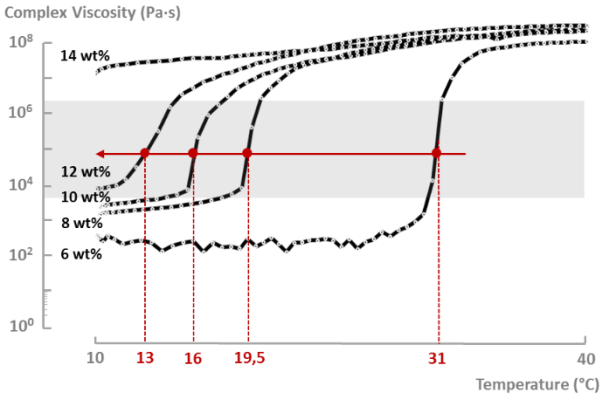

Figure 2. Complex viscosity (log scale) as a function of temperature based on rheological experiments; gelation: at lower temperatures for higher PNIPAM concentrations and determining the ideal viscosity range for electrospinning (highlighted in grey: see Section Design of electrospinning conditions).

The temperature at which the highest change in complex viscosity occurs, is chosen as an indication for gelation.[59–61] This temperature is in good agreement with the crossover temperature of the loss and storage modulus, as given in Figure 3.

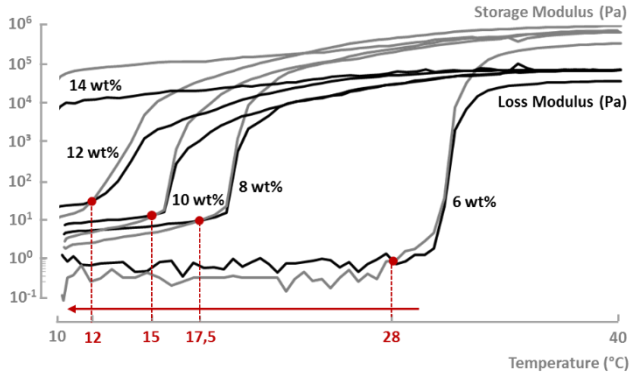

Figure 3. The crossover of loss and storage modulus (log scale), *i.e.* gel point, is located at lower temperatures for increasing concentrations.

A clear dependence of the complex viscosity on the solution temperature is observed. Below a certain threshold temperature, here called the gelation temperature, the loss modulus is at a given mass concentration always higher than the storage modulus (Figure 2 and 3), meaning that the polymer solution behaves as a viscoelastic liquid. At higher temperatures, it is thermodynamically more favorable for the polymer chains to interact with themselves due to partial dehydration. This initiates physical crosslinking and, thus, an increase in viscosity eventually resulting in gelation, which is reflected by a drastic increase in complex viscosity (Figure 2). Above this gelation temperature, the storage modulus dominates the loss modulus (Figure 3), meaning that the polymer solution behaves now as a viscoelastic solid gel that is no longer suited for stable electrospinning.

Very remarkable is the effect of the mass concentration on the gelation temperature, which significantly decreases with increasing polymer concentration. For the 6 wt% polymer solutions, the gelation temperature more or less coincides with the T_{CP} of PNIPAM as measured by

turbidimetry above (Figure 1; 31 °C). This means that a gel is formed at the T_{CP}, followed by immediate demixing of the solution. This fast dehydration behavior was also observed for low concentration polyisocyanopeptide hydrogels.[68] In contrast to the 6 wt% solutions, the gelation temperature for the higher PNIPAM concentrations is significantly lower than the T_{CP} and this difference increases with increasing mass concentration. For example, at 8 wt% the difference amounts to ± 12 °C whereas at 12 wt% this difference is already ± 17 °C. This indicates that, at the higher polymer concentrations, partial dehydration of the polymer chains below the T_{CP} can already induce sufficient interchain interactions to form a clear transparent gel structure. It should be noted that, at this temperature, no formation of particles or other agglomerates due to phase separation were observed. Only when the T_{CP} is reached at higher temperatures, further dehydration leads to the collapse and phase separation of the PNIPAM chains into non-soluble globule-like structures, which results in the formation of opaque gels. Note that in the case of high mass concentrations (*e.g.* 14 wt% solutions), the polymer solution is already in the gel state at 10 °C.

For electrospinning, this phenomenon of gelation prior to the T_{CP} is extremely important. Firstly, it indicates that the viscosity of the polymer solution highly depends on both temperature and concentration. Secondly, and more importantly, it also shows that for higher PNIPAM concentrations, important rheological changes are manifested before the LCST transition, which are expected to be crucial for PNIPAM's electrospinnability. Above the gelation temperature, the PNIPAM solution consists of physically crosslinked solid gels characterized by too low flowability to form uniform, bead-free nanofibers. Around the gelation temperature, the viscosity is lower, yet high enough to result in a stable electrospinning in case the mass concentration is controlled (see further). Hence, only at specific concentrations at which the gelation temperature is significantly

below the T_{CP}, good solubility is combined with the required viscosity range for electrospinning. Under such premises a solution temperature can be found at which both solubility and viscosity are suited for a stable electrospinning process to occur.

In summary, the turbidity and rheological results show that for electrospinnability not only the T_{CP}, which is related to PNIPAM's solubility should be considered. In addition, also the concentration-dependent rheological behavior of the solution prior to the LCST-transition should be taken into account as this will determine the appropriate viscosity range. Moreover, for each polymer concentration, this viscosity range is located at a different temperature. This environmental parameter should, thus, be controlled to obtain a stable electrospinning process. Therefore, all electrospinning solutions stated in Table 1 are electrospun under acclimatized conditions.

3.2 Relevance of relative humidity control

In addition to the temperature, also the relative humidity needs to be controlled during electrospinning, as it influences the evaporation and transport of water. DVS analysis (Figure 4 top; 20 °C) indicates a much slower evaporation of water molecules from the PNIPAM solutions in case of a higher relative humidity, which explains poor electrospinnability under these conditions (Figure 5). At a low relative humidity, *i.e.* below 35 %RH, an increase in temperature (17 to 24 °C) further enhances the evaporation and transport of water (Figure 4 bottom).

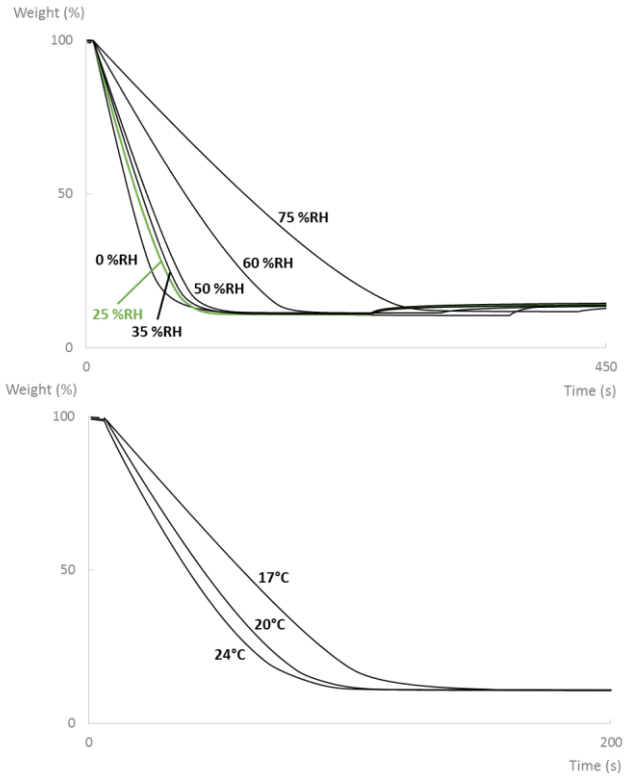

Figure 4. DVS shows that a relative humidity below 35% speeds up the water evaporation and transport of a 10 wt% electrospinning solution at 20 °C (top). At such a low relative humidity (25 %RH, bottom) an increase in the environmental temperature fastens the water evaporation and transport.

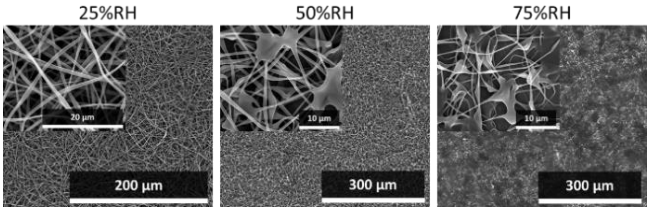

Figure 5. SEM images of 8 wt% PNIPAM nanofibers after electrospinning at different relative humidity, clearly showing non-uniformity and beads at increasing relative humidity. Temperature was kept constant at 20 °C based on the rheological results in Figure 2 and 3.

These results indicate that, for electrospinnability, the relative humidity should be kept as low as possible, taking into account practical constraints. Therefore, all further experiments have been performed at a relative humidity of 25 ± 5 %RH. High temperatures (> 20°C) are also favorable for the electrospinning process in terms of solvent evaporation. However, as discussed above (Figure 2 and 3), a too high temperature can be accompanied by a too high viscosity and a limiting temperature is thus expected.

For stable electrospinning, it can be concluded that it is crucial to determine the optimal temperature and concentration window at a low RH, as explored in the next section.

3.4 Design of electrospinning conditions

Figure 6 shows an overview of the nanofibers electrospun from different PNIPAM concentrations (6-14 wt%) in water at different temperatures (17-32°C), all at a relative humidity of 25 ± 5 %RH to ensure a sufficiently fast water evaporation (Figure 4).

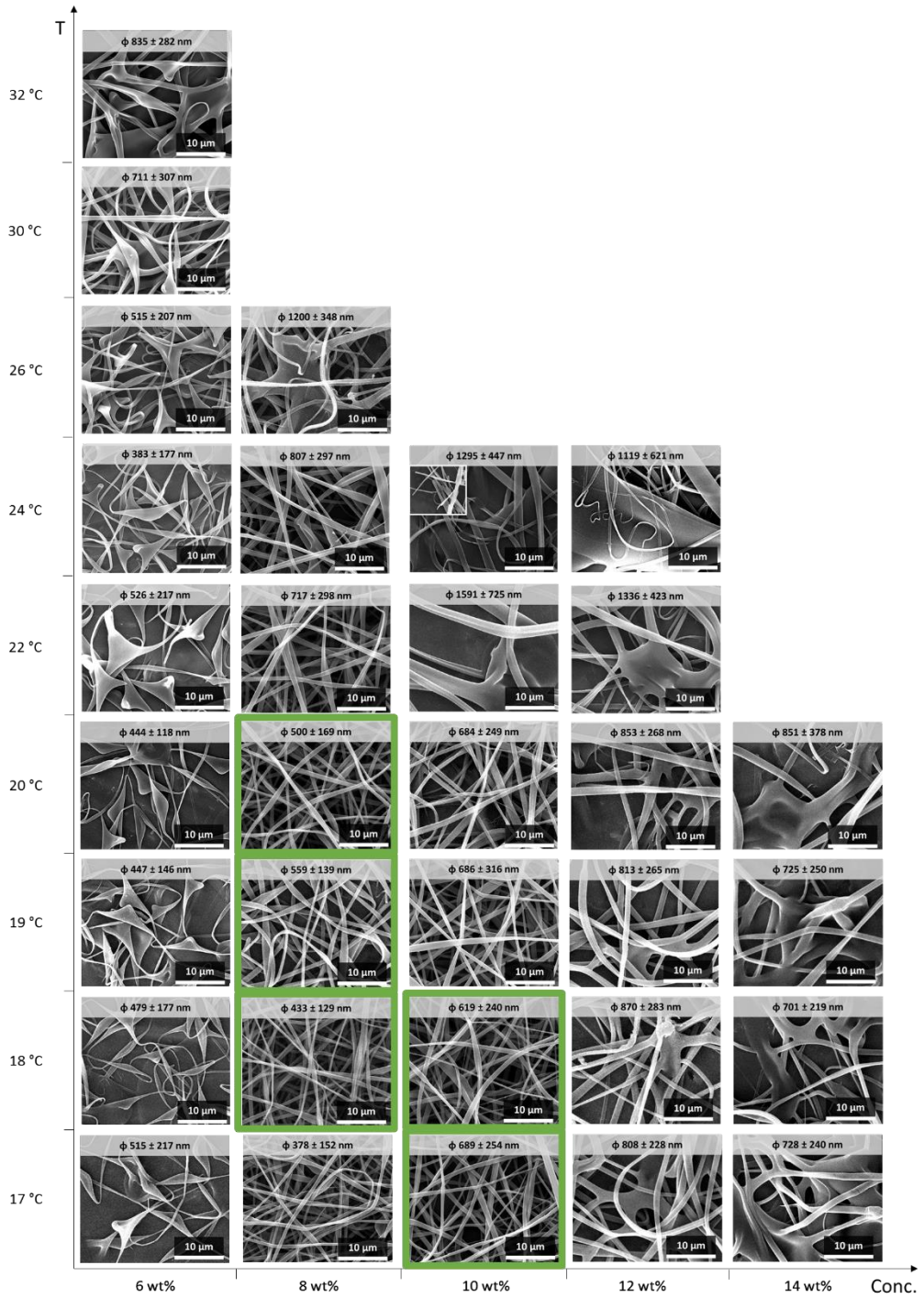

Figure 6. SEM-images of the produced nanofibers from different PNIPAM concentrations and at different solution temperatures show that electrospinnability depends on both parameters (25 ± 5 %RH). Best electrospinning conditions resulting in uniform, bead-less nanofibers are highlighted in green.

At a concentration of 6 wt% the amount of water is too high and the viscosity too low at the lower to intermediate temperatures (< 30°C) to form uniform nanofibers. As the temperature of gelation coincides with the T_{CP} (Figure 2; 31°C), a higher temperature does not only result in a higher viscosity, which might be appropriate for electrospinning, but also causes undesired demixing of the solution.

A close inspection of the first column in Figure 6 shows that these low polymer mass concentrations lead to non-uniform so-called barbed fibers. Together with beads, triangle-shaped branches are being formed. At a concentration of 7 wt% PNIPAM the beads disappear and the triangle-shaped branches appear more regularly (Figure 7). Holzmeister *et al.* reported a similar morphology for polyvinylalcohol spun from water and named the branches barbed fibers. These novel and unique type of nanofibers could pave the way towards new applications, *e.g.* inhalation therapy and fiber reinforcement, as they clearly differ from ordinary uniform nanofibers.[51,69,70]

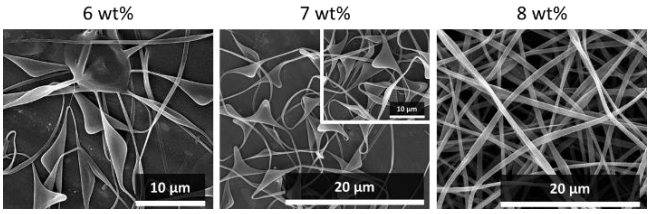

Figure 7. SEM images of 6 wt%, 7 wt% and 8 wt% nanofibers electrospun at 20 °C and 25 ± 5 %RH. 6 - 7 wt% provides ideal conditions for the formation of barbed nanofibers, whereas 8 wt% provides ideal conditions for the formation of uniform, continuous nanofibers.

For the formation of uniform, bead-free nanofibers, intermediate concentrations of 8 and 10 wt% PNIPAM show the best electrospinning results (Figure 6). However, as the concentration increases from 8 to 10 wt%, process stability is limited by a decrease in the limiting temperature from 24 °C to 20 °C. Nozzle-clogging appears and non-uniform nanofibers arise together with a lot of beads,

once the temperature passes the respective threshold. In case of the 8 wt% solutions, the optimal feasible temperature range for electrospinning appears to be 18 °C - 20 °C. This temperature range is lowered to 17°C – 18 °C in case of the 10 wt% solutions. Solutions of 12 wt% PNIPAM still result in nanofibers, however, electrospinning is less stable as nozzle-clogging occurred, the nanofibers are less uniform, more beads are present and the nanofibers are characterized by a larger diameter. Completely unstable electrospinning is obtained as soon as the PNIPAM concentration reaches 14 wt%.

These results clearly reflect the crucial influence of the temperature- and concentration-dependent rheological behavior of PNIPAM on its electrospinnability, as discussed above. Indeed, the results confirm that PNIPAM is electrospinnable from water, but only at concentrations where gelation occurs at feasible electrospinning temperatures that are significantly lower than the T_{CP}. A specific temperature range thus exists where good solubility is combined with viscosities that allow for stable electrospinning.

In case of the 8 wt% solutions, gelation occurs between 18 °C and 20 °C, which is significantly lower than the T_{CP} of *ca.* 31 °C (Figure 1). A transparant "gel" is, thus, formed, which is accompanied by an increase in viscosity. Within this temperature range just before solidification, the viscosity is sufficiently high to form nanofibers, yet low enough to maintain a stable electrospinning process (highlighted in grey in Figure 2). As can be seen from Figure 6, this temperature range provides nice, uniform, bead-less nanofibers. If the environmental temperature is further increased, the amount of physical crosslinking is also increased, which is accompanied by a higher viscosity, resulting in larger nanofiber diameters. Eventually, this results in an unstable electrospinning process accompanied with nozzle-clogging. For the 10 wt% PNIPAM concentrations, rheological measurements show that physical crosslinking starts at lower

temperatures, *i.e.* 16 °C – 18°C (Figure 2). Again, a transparant "gel" is formed, but at a lower temperature. This means that the ideal viscosity range for stable electrospinning is shifted to a lower temperature range. Indeed, within the feasible electrospinning temperature range of 17 °C – 18 °C, 10 wt% PNIPAM solutions show excellent electrospinnability. From 20 °C, physical crosslinking has developed too extensively, resulting in too high viscosities. This, again, leads to nozzle-clogging and eventually an unstable electrospinning process. For the higher concentrations, *i.e.* 12 wt% and 14 wt%, gelation is initiated even at lower temperatures, moving the ideal viscosity range for PNIPAM electrospinning further downwards, out of the feasible electrospinning temperature range as determined by equipment limitations.

In summary, within the concentration range 8 – 10 wt%, aqueous PNIPAM solutions show the ideal circumstances for excellent electrospinnability from water. Gelation occurs at a significantly lower temperature than PNIPAM's LCST, which means that the viscosity of the solution increases, without reducing the solubility of the polymer chains. Moreover, this temperature is still high enough to allow for a practically feasible electrospinning process. If the environmental temperature and relative humidity are controlled during the process, optimal conditions have been identified to allow for the production of uniform, continuous, bead-less nanofibers by waterborne electrospinning.

As a proof-of-principle to show the potential of waterborne electrospinning of PNIPAM nanofibers for biomedical applications, fluorescein was incorporated as biorelevant compound in the nanofibrous membranes by dye-doping. A concentration of 0.5 wt% (on polymer mass) fluorescein was added to a 10 wt% PNIPAM aqueous solution and consequently electrospun at the optimal electrospinning conditions for 10 wt% solutions as determined above. Although the viscosity of the polymer solution was increased upon addition of the dye and the process needs

further optimization, uniform, bead-less nanofibers were obtained, which showed the characteristic fluorescence of fluorescein (Figure 8 and ESI Figure S5). A biorelevant model compound such as fluorescein can, thus, be introduced in the nanofibers without compromising significantly the nanofiber morphology nor the electrospinning process while preserving the fluorescent character of the compound.

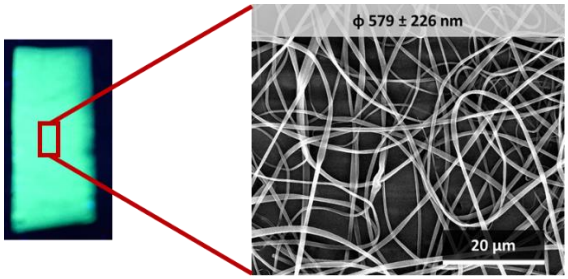

Figure 8. 10 wt% PNIPAM nanofibers doped with fluorescein show nice yellow/green fluorescence when viewed under UV-light (λ_{ext}-336 nm). Doping of this fluorescent dye into the nanofibers leaves the nanofiber morphology as well as the fluorescent character of the compound intact.

3.5 Water stability testing

What makes PNIPAM so interesting for many applications is its solubility in water below its LCST, yet water stability above this temperature. This means that PNIPAM can be processed from water at low temperatures, as discussed above, but can be applied as a water-stable material at higher temperatures. For many nanofibrous applications, this water stability is a highly desired feature. In order to test the water stability of the PNIPAM nanofibers, the produced nanofibrous membranes are immersed in water at temperatures above PNIPAM's LCST. After immersion, the samples are dried at 90 °C, which is well below the glass transition temperature of PNIPAM, in order to perform SEM-analysis. As can be seen in Figure 9 and Figure 10, both after immersion in water at 37 °C and 50 °C the nanofibrous structure remains.

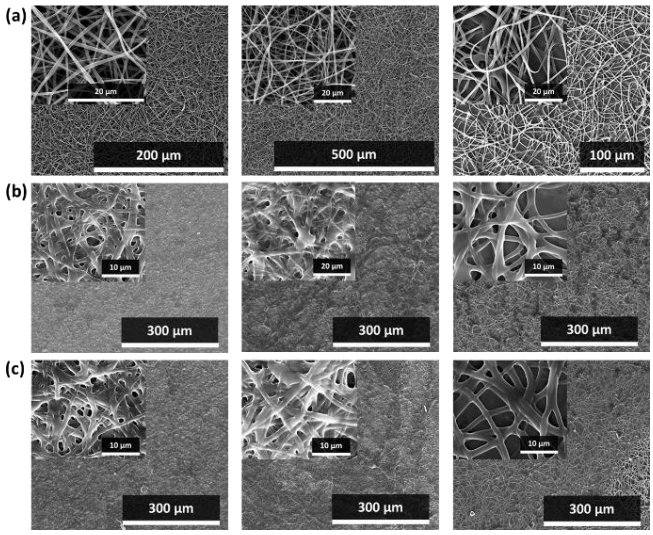

Figure 9. Water stability tests of the produced nanofibers containing 8 wt%, 10 wt% and 12 wt% PNIPAM (left to right) show that the nanofibrous structure remains intact at 50 °C, albeit with some swelling due to water absorption. (a) Before immersion, (b) after 30 seconds of immersion, (c) after 5 minutes of immersion.

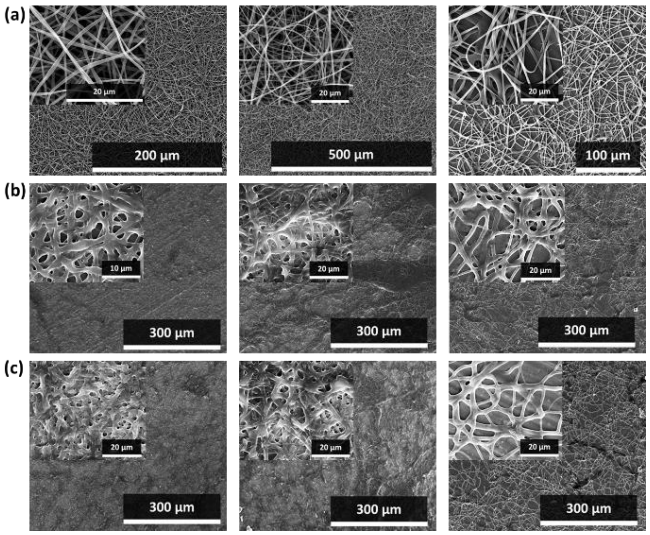

Figure 10. Water stability tests of the produced nanofibers containing 8 wt%, 10 wt% and 12 wt% PNIPAM (left to right) show that the nanofibrous structure remains intact at 37 °C, albeit with some swelling due to water absorption. (a) Before immersion, (b) after 30 seconds of immersion, (c) after 5 minutes of immersion.

No dissolution occurs, yet some swelling is observed due to unavoidable interactions with the water molecules. The 12 wt% samples seem to be more resistant to this swelling, possibly because these nanofibers possess larger nanofiber diameters, as can be seen from Figure 6, making them more robust. In contrast, samples that are immersed in water at temperatures below 31 °C, *i.e.* below the T_{CP} of PNIPAM, are completely and immediately dissolved in water, as expected indicating the switchable aqueous solubility of these PNIPAM nanofibers.

4 Conclusions and future outlook

Water-stable, well-defined, continuous, uniform, and bead-less PNIPAM nanofibers can be produced by waterborne electrospinning, facilitated by the rise in solution viscosity at temperatures significantly lower than the T_{CP}, which was found to be the case for higher concentrated PNIPAM solutions.

It is reported that for concentrations around 8 wt%, PNIPAM shows gelation at significantly lower temperatures than the LCST, resulting in a clear, transparent gel-like structure. This phenomenon proved to be crucial for PNIPAM's electrospinnability as it provides a concentration-dependent temperature range around the gelation temperature, wherein good solubility is combined with an increased viscosity that is suited for stable electrospinning from water. Although majorly overlooked in literature today, it is therefore crucial to adjust and control the environmental temperature as such. Moreover, also the relative humidity proved to play a crucial role, as a lower relative humidity (25 % RH) allows for a sufficiently fast water evaporation, required to form uniform nanofibers.

It can be expected that these insights will not only apply to the electrospinning of PNIPAM but also to the electrospinnability of its related copolymers and other thermoresponsive (co)polymers. This hypothesis as well as the investigation of different molecular weights and the influence of

salts, which are known to influence the LCST behavior of PNIPAM, will be the focus of future research. Nevertheless, the current results already provide important insights in the rheological behavior of the thermoresponsive polymer PNIPAM and its electrospinnability from water, showing major potential to many applications in biomedicine, including drug delivery and cell culture.

5 Acknowledgments

Financial support from the Research Foundation of Flanders (FWO) and the Agency for Innovation by Science and Technology of Flanders (IWT) is gratefully acknowledged. Results in this paper were obtained within the framework of the FWO Strategic Basic Research grant 1S05517N and the IWT Strategic Basic Research grants 121241, S.M., D.R.D. and P.H.M.V.S. acknowledge the FWO through a postdoctoral fellowship.

6 Supporting Information. Figure S1: DSC traces of commercial PNIPAM powder and produced PNIPAM nanofibers. Figure S2: SEM images of produced PNIPAM nanofibers which were dried or not dried after electrospinning. Figure S3: SEM images of PNIPAM nanofibers after waterstability tests with different drying procedures. Figure S4: Fluorescence spectrum of PNIPAM nanofibers doped with fluorescein.

7 References

(1) Zhernenkov, M.; Ashkar, R.; Feng, H.; Akintewe, O. O.; Gallant, N. D.; Toomey, R.; Ankner, J. F.; Pynn, R. Thermoresponsive PNIPAM Coatings on Nanostructured Gratings for Cell Alignment and Release. *ACS Appl. Mater. Interfaces* **2015**, *7* (22), 11857–11862.

(2) Stile, R. A.; Healy, K. E. Thermo-Responsive Peptide-Modified Hydrogels for Tissue

Regeneration. *Biomacromolecules* **2001**, *2* (1), 185–194.

(3) Ward, M. A.; Georgiou, T. K. Thermoresponsive Polymers for Biomedical Applications. *Polymers (Basel)*. **2011**, *3* (3), 1215–1242.

(4) Guan, Y.; Zhang, Y. PNIPAM Microgels for Biomedical Applications: From Dispersed Particles to 3D Assemblies. *Soft Matter* **2011**, *7* (14), 6375.

(5) Nolan, C. M.; Serpe, M. J.; Lyon, L. A. Thermally Modulated Insulin Release from Microgel Thin Films. *Biomacromolecules* **2004**, *5* (5), 1940–1946.

(6) Islam, M. R.; Ahiabu, A.; Li, X.; Serpe, M. J. Poly (N-Isopropylacrylamide) Microgel-Based Optical Devices for Sensing and Biosensing. *Sensors (Basel)*. **2014**, *14* (5), 8984–8995.

(7) Schild, H. G. Poly (N-Isopropylacrylamide): Experiment , Theory and Application. *Prog. Polym. Sci.* **1992**, *17* (2), 163–249.

(8) Hacker, M. C.; Klouda, L.; Ma, B. B.; Kretlow, J. D.; Mikos, A. G. Synthesis and Characterization of Injectable, Thermally and Chemically Gelable, Amphiphilic poly(N-Isopropylacrylamide)-Based Macromers. *Biomacromolecules* **2008**, *9* (6), 1558–1570.

(9) Twaites, B. R.; De Las Heras Alarcón, C.; Lavigne, M.; Saulnier, A.; Pennadam, S. S.; Cunliffe, D.; Górecki, D. C.; Alexander, C. Thermoresponsive Polymers as Gene Delivery Vectors: Cell Viability, DNA Transport and Transfection Studies. *J. Control. Release* **2005**, *108* (2–3), 472–483.

(10) Ganta, S.; Devalapally, H.; Shahiwala, A.; Amiji, M. A Review of Stimuli-Responsive Nanocarriers for Drug and Gene Delivery. *Journal of Controlled Release*. 2008, pp 187–

204.

(11) Miyata, K.; Christie, R. J.; Kataoka, K. Polymeric Micelles for Nano-Scale Drug Delivery. *React. Funct. Polym.* **2011**, *71* (3), 227–234.

(12) Maji, S.; Cesur, B.; Zhang, Z.; De Geest, B.; Hoogenboom, R. Poly(N-Isopropylacrylamide) Coated Gold Nanoparticles as Colourimetric Temperature and Salt Sensors. *Polym. Chem.* **2016**, *7* (Scheme 1), 1705–1710.

(13) Vancoillie, G.; Zhang, Q.; Hoogenboom, R. Chapter 7. Polymeric Temperature Sensors; 2016; pp 190–236.

(14) Hu, J.; Liu, S. Responsive Polymers for Detection and Sensing Applications: Current Status and Future Developments. *Macromolecules* **2010**, *43* (20), 8315–8330.

(15) Tzeng, P.; Kuo, C.-C.; Lin, S.-T.; Chiu, Y.-C.; Chen, W.-C. New Thermoresponsive Luminescent Electrospun Nanofibers Prepared from Poly[2,7-(9,9-Dihexylfluorene)]-Block-poly(N-isopropylacrylamide)/PMMA Blends. *Macromol. Chem. Phys.* **2010**, *211* (13), 1408–1416.

(16) Muthiah, P.; Hoppe, S. M.; Boyle, T. J.; Sigmund, W. Thermally Tunable Surface Wettability of Electrospun Fiber Mats: polystyrene/poly(N-Isopropylacrylamide) Blended versus Crosslinked poly[(N-Isopropylacrylamide)-Co-(Methacrylic Acid)]. *Macromol. Rapid Commun.* **2011**, *32* (21), 1716–1721.

(17) Umapathi, R.; Reddy, P. M.; Kumar, A.; Venkatesu, P.; Chang, C.-J. The Biological Stimuli for Governing the Phase Transition Temperature of The “smart” polymer PNIPAM in Water. *Colloids Surf. B. Biointerfaces* **2015**, *135*, 588–595.

(18) Afroze, F.; Nies, E.; Berghmans, H. Phase Transitions in the System poly(N-Isopropylacrylamide)/water and Swelling Behaviour of the Corresponding Networks. *J. Mol. Struct.* **2000**, *554* (1), 55–68.

(19) Baysal, B. M.; Karasz, F. E. Coil-Globule Collapse in Flexible Macromolecules. *Macromolecular Theory and Simulations*. WILEY- VCH Verlag December 2003, pp 627–646.

(20) Costa, R. O. .; Freitas, R. F. . Phase Behavior of poly(N-Isopropylacrylamide) in Binary Aqueous Solutions. *Polymer (Guildf).* **2002**, *43* (22), 5879–5885.

(21) De La Rosa, V. R.; Woisel, P.; Hoogenboom, R. Supramolecular Control over Thermoresponsive Polymers. *Materials Today*. 2016, pp 44–55.

(22) Graziano, G. On the Temperature-Induced Coil to Globule Transition of Poly-N-Isopropylacrylamide in Dilute Aqueous Solutions. *International Journal of Biological Macromolecules*. March 2000, pp 89–97.

(23) Halperin, A.; Kröger, M.; Winnik, F. M. Poly(N-Isopropylacrylamide) Phase Diagrams: Fifty Years of Research. *Angew. Chemie - Int. Ed.* **2015**, *54* (51), 15342–15367.

(24) da Silva, R. M. P.; Mano, J. F.; Reis, R. L. Smart Thermoresponsive Coatings and Surfaces for Tissue Engineering: Switching Cell-Material Boundaries. *Trends in Biotechnology*. 2007, pp 577–583.

(25) Yamada, N.; Okano, T.; Sakai, H.; Karikusa, F.; Sawasaki, Y.; Sakurai, Y. Thermo-Responsive Polymeric Surfaces; Control of Attachment and Detachment of Cultured Cells. *Die Makromol. Chemie, Rapid Commun.* **1990**, *11* (11), 571–576.

(26) Kikuchi, A.; Okano, T. Nanostructured Designs of Biomedical Materials: Applications of Cell Sheet Engineering to Functional Regenerative Tissues and Organs. In *Journal of Controlled Release*; 2005; Vol. 101, pp 69–84.

(27) Peter X.MA. Tissue Engineering. *Encycl. Polym. Sci. Technol.* **2004**, *12* (3).

(28) Fang, J.; Wang, X.; Lin, T. Functional Applications of Electrospun Nanofibers. *Nanofibers - Prod. Prop. Funct. Appl.* **2011**, 287–326.

(29) Zeng, J.; Xu, X.; Chen, X.; Liang, Q.; Bian, X.; Yang, L.; Jing, X. Biodegradable Electrospun Fibers for Drug Delivery. *J. Control. Release* **2003**, *92* (3), 227–231.

(30) Zeng, J.; Yang, L.; Liang, Q.; Zhang, X.; Guan, H.; Xu, X.; Chen, X.; Jing, X. Influence of the Drug Compatibility with Polymer Solution on the Release Kinetics of Electrospun Fiber Formulation. *J. Control. Release* **2005**, *105* (1–2), 43–51.

(31) Ramakrishna, S.; Fujihara, K.; Teo, W. E.; Yong, T.; Ma, Z.; Ramaseshan, R. Electrospun Nanofibers: Solving Global Issues. *Mater. Today* **2006**, *9* (3), 40–50.

(32) Vasita, R.; Katti, D. S. Nanofibers and Their Applications in Tissue Engineering. *International Journal of Nanomedicine*. Dove Press 2006, pp 15–30.

(33) Goh, Y.-F.; Shakir, I.; Hussain, R. Electrospun Fibers for Tissue Engineering, Drug Delivery, and Wound Dressing. *J. Mater. Sci.* **2013**, *48* (8), 3027–3054.

(34) Agarwal, S.; Burgard, M.; Greiner, A.; Wendorff, J. *Electrospinning: A Practical Guide to Nanofibers*; De Gruyter Textbook; De Gruyter, 2016.

(35) Schoolaert, E.; Steyaert, I.; Vancoillie, G.; Geltmeyer, J.; Lava, K.; Hoogenboom, R.; De

Clerck, K. Blend Electrospinning of Dye-Functionalized Chitosan and Poly(ε-Caprolactone): Towards Biocompatible pH-Sensors. *J. Mater. Chem. B* **2016**, *4* (26), 4507–4516.

(36) Wang, X.; Drew, C.; Lee, S.-H.; Senecal, K. J.; Kumar, J.; Samuelson, L. A. Electrospun Nanofibrous Membranes for Highly Sensitive Optical Sensors. *Nano Lett.* **2002**, *2* (11), 1273–1275.

(37) Geltmeyer, J.; Vancoillie, G.; Steyaert, I.; Breyne, B.; Cousins, G.; Lava, K.; Hoogenboom, R.; De Buysser, K.; De Clerck, K. Dye Modification of Nanofibrous Silicon Oxide Membranes for Colorimetric HCl and NH3 Sensing. *Adv. Funtional Mater.* **2016**.

(38) Andrady, L. A. *Science and Technology of Polymer Nanofibers*; 2008.

(39) Steyaert, I.; Rahier, H.; De Clerck, K. Nanofibre-Based Sensors for Visual and Optical Monitoring. In *Electrospinning for High Performance Sensors*; Macagnano, A., Zampetti, E., Kny, E., Eds.; 2015; pp 157–177.

(40) Slemming-Adamsen, P.; Song, J.; Dong, M.; Besenbacher, F.; Chen, M. In Situ Cross-Linked PNIPAM/Gelatin Nanofibers for Thermo-Responsive Drug Release. *Macromol. Mater. Eng.* **2015**, *300* (12), 1226–1231.

(41) Prabaharan, M.; Jayakumar, R.; Nair, S. V. Electrospun Nanofibrous Scaffolds-Current Status and Prospects in Drug Delivery. In *Biomedical Applications of Polymeric Nanofibers*; Jayakumar, R., Nair, S., Eds.; Springer Berlin Heidelberg: Berlin, Heidelberg, 2012; pp 140–262.

(42) Bhardwaj, N.; Kundu, S. C. Electrospinning: A Fascinating Fiber Fabrication Technique.

Biotechnol. Adv. **2010**, *28* (3), 325–347.

(43) Ramakrishna, S. *An Introduction to Electrospinning And Nanofibers (Google eBook)*; World Scientific, 2005.

(44) Sun, J.; Bubel, K.; Chen, F.; Kissel, T.; Agarwal, S.; Greiner, A. Nanofibers by Green Electrospinning of Aqueous Suspensions of Biodegradable Block Copolyesters for Applications in Medicine, Pharmacy and Agriculture. *Macromol. Rapid Commun.* **2010**, *31* (23), 2077–2083.

(45) Wang, C.; Wang, Y.; Hashimoto, T. Impact of Entanglement Density on Solution Electrospinning: A Phenomenological Model for Fiber Diameter. *Macromolecules* **2016**, *49* (20), 7985–7996.

(46) Persano, L.; Camposeo, A.; Tekmen, C.; Pisignano, D. Industrial Upscaling of Electrospinning and Applications of Polymer Nanofibers: A Review. *Macromol. Mater. Eng.* **2013**, *298* (5), 504–520.

(47) Agarwal, S.; Greiner, A. On the Way to Clean and Safe Electrospinning-Green Electrospinning: Emulsion and Suspension Electrospinning. *Polymers for Advanced Technologies*. John Wiley & Sons, Ltd. March 2011, pp 372–378.

(48) Chen, H.; Hsieh, Y. Lo. Ultrafine Hydrogel Fibers with Dual Temperature- and pH-Responsive Swelling Behaviors. *J. Polym. Sci. Part A Polym. Chem.* **2004**, *42* (24), 6331–6339.

(49) Hoffman, A. S. “Intelligent” Polymers in Medicine and Biotechnology. *Artif. Organs* **1995**, *19* (5), 458–467.

(50) Okuzaki, H.; Kobayashi, K.; Yan, H. Non-Woven Fabric of poly(N-Isopropylacrylamide) Nanofibers Fabricated by Electrospinning. *Synth. Met.* **2009**, *159* (21), 2273–2276.

(51) Rockwood, D. N.; Chase, D. B.; Akins, R. E.; Rabolt, J. F. Characterization of Electrospun poly(N-Isopropyl Acrylamide) Fibers. *Polymer (Guildf).* **2008**, *49* (18), 4025–4032.

(52) Song, F.; Wang, X. L.; Wang, Y. Z. Poly (N-Isopropylacrylamide)/poly (Ethylene Oxide) Blend Nanofibrous Scaffolds: Thermo-Responsive Carrier for Controlled Drug Release. *Colloids Surfaces B Biointerfaces* **2011**, *88* (2), 749–754.

(53) Lin, X.; Tang, D.; Cui, W.; Cheng, Y. Controllable Drug Release of Electrospun Thermoresponsive poly(N-isopropylacrylamide)/poly(2-Acrylamido-2-Methylpropanesulfonic Acid) Nanofibers. *J. Biomed. Mater. Res. - Part A* **2012**, *100 A* (7), 1839–1845.

(54) Saithongdee, A.; Varanusupakul, P.; Imyim, A. Preparation of Thermally Sensitive poly[N-Isopropylacrylamide-Co-(Maleic Acid)] Hydrogel Membrane by Electrospinning Using a Green Solvent. *Green Chem. Lett. Rev.* **2014**, *7* (3), 220–227.

(55) Salehi, R.; Irani, M.; Rashidi, M.-R.; Aroujalian, A.; Raisi, A.; Eskandani, M.; Haririan, I.; Davaran, S. Stimuli-Responsive Nanofibers Prepared from poly(N-Isopropylacrylamide-Acrylamide-Vinylpyrrolidone) by Electrospinning as an Anticancer Drug Delivery. *Des. Monomers Polym.* **2013**, *16* (6), 515–527.

(56) Song, F.; Wang, X.-L.; Wang, Y.-Z. Fabrication of Novel Thermo-Responsive Electrospun Nanofibrous Mats and Their Application in Bioseparation. *Eur. Polym. J.* **2011**, *47* (10), 1885–1892.

(57) Tran, T.; Hernandez, M.; Patel, D.; Wu, J. Temperature and pH Responsive Microfibers for Controllable and Variable Ibuprofen Delivery. *Adv. Mater. Sci. Eng.* **2015**, *2015*, 6.

(58) Wang, J.; Sutti, A.; Wang, X.; Lin, T. Fast Responsive and Morphologically Robust Thermo-Responsive Hydrogel Nanofibres from poly(N-Isopropylacrylamide) and POSS Crosslinker. *Soft Matter* **2011**, *7* (9), 4364.

(59) Munk, T.; Hietala, S.; Kalliomaki, K.; Nuopponen, M.; Tenhu, H.; Tian, F.; Rantanen, J.; Baldursdottir, S. Rheological Behaviour of Poly(N-Isopropyl Acrylamide) in Water-Acetone Mixtures. *Annu. Trans. Nord. Rheol. Soc.* **2009**, *17*.

(60) Antunes, F. E.; Gentile, L.; Tavano, L.; Rossi, C. O. Rheological Characterization of the Thermal Gelation of poly(N-Isopropylacrylamide) and poly(N-Isopropylacrylamide)co-Acrylic Acid. *Appl. Rheol.* **2009**, *19* (4), 42064–42069.

(61) Winter, H. H. Can the Gel Point of a Crosslinking Polymer Be Detected by the G'-G" crossover? *Polymer Engineering and Science*. Society of Plastics Engineers December 1987, pp 1698–1702.

(62) Zhang, Q.; Weber, C.; Schubert, U. S.; Hoogenboom, R. Thermoresponsive Polymers with Lower Critical Solution Temperature: From Fundamental Aspects and Measuring Techniques to Recommended Turbidimetry Conditions. *Mater. Horiz.* **2017**, *4* (2), 109–116.

(63) Boutris, C.; Chatzi, E. G.; Kiparissides, C. Characterization of the LCST Behaviour of Aqueous poly(N-Isopropylacrylamide) Solutions by Thermal and Cloud Point Techniques. *Polymer (Guildf).* **1997**, *38* (10), 2567–2570.

(64) Heskins, M.; Guillet, J. E. Solution Properties of Poly(N-Isopropylacrylamide). *J. Macromol. Sci. Part A - Chem.* **1968**, *2* (8), 1441–1455.

(65) Van Durme, K.; Rahier, H.; Van Mele, B. Influence of Additives on the Thermoresponsive Behavior of Polymers in Aqueous Solution. *Macromolecules* **2005**, *38* (24), 10155–10163.

(66) Wintgens, V.; Amiel, C. Physical Gelation of Amphiphilic poly(N-Isopropylacrylamide): Influence of the Hydrophobic Groups. *Macromol. Chem. Phys.* **2008**, *209* (15), 1553–1563.

(67) Zheng, X.; Tong, Z.; Xie, X.; Zeng, F. Phase Separation in Poly(N-Isopropyl acrylamide)/Water Solutions I. Cloud Point Curves and Microgelation. *Polym. J.* **1998**, *30* (4), 284–288.

(68) Kouwer, P. H. J.; Koepf, M.; Le Sage, V. A. A.; Jaspers, M.; van Buul, A. M.; Eksteen-Akeroyd, Z. H.; Woltinge, T.; Schwartz, E.; Kitto, H. J.; Hoogenboom, R.; Picken, S. J.; Nolte, R. J. M.; Mendes, E.; Rowan, A. E. Responsive Biomimetic Networks from Polyisocyanopeptide Hydrogels. *Nature* **2013**, *493* (7434), 651–655.

(69) Holzmeister, A.; Yarin, A. L.; Wendorff, J. H. Barb Formation in Electrospinning: Experimental and Theoretical Investigations. *Polymer (Guildf).* **2010**, *51* (12), 2769–2778.

(70) Holzmeister, A.; Grelner, A.; Wendorff, J. H. “Barbed Nanowires” from Polymers Wia Electrospinning. *Polym. Eng. Sci.* **2009**, *49* (1), 148–153.

For Table of Contents use only

Waterborne Electrospinning of poly(*N*-isopropyl acrylamide) by control of environmental parameters

Ella Schoolaert, Paulien Ryckx, Jozefien Geltmeyer, Samarendra Maji, Paul H.M. Van Steenberge, Dagmar R. D'hooge, Richard Hoogenboom and Karen De Clerck